Journal of Coastal Research	17	1	195–206	West Palm Beach, Florida	Winter 2001

Field Measurements of Sediment Dynamics in Front of a Seawall

Jonathon R. Miles, Paul E. Russell and David A. Huntley

Institute of Marine Studies
University of Plymouth
Drake Circus
Devon, PL4 8AA U.K.

ABSTRACT

MILES, J.R.; RUSSELL, P.E., and HUNTLEY, D.A., 2001. Field Measurements of Sediment Dynamics in Front of a Seawall. *Journal of Coastal Research,* 17(1), 195–206. West Palm Beach (Florida), ISSN 0749-0208.

A field experiment has been carried out to examine the effects of seawalls on hydrodynamic and sediment dynamic processes on sandy beaches. Pressure transducers, electromagnetic current meters and optical backscatter sensors were deployed directly in front of a seawall at Teignmouth, South Devon (U.K.) in June 1995. Similar instruments were deployed simultaneously on the adjacent natural beach.

Reflection coefficients were in the range 0.7 to 1.0 at the wall and around 0.2 on the natural beach for incident wave frequencies (0.125–0.36 Hz). Reflection coefficients at lower frequencies (0.04–0.125 Hz), were close to unity at the wall, whilst on the beach the reflection coefficient increased with decreasing frequency, reaching 0.9 at the low frequency spectral peak.

Both sediment suspension and transport were altered significantly by the presence of the wall. Mean suspended sediment concentrations were found to be up to three times larger in front of the wall than on the natural beach. This increase was attributed to the increase in wave reflection. The largest differences occurred when the waves were largest, and the water was shallow. A net onshore sediment transport by incident waves was observed on the natural beach. In front of the wall, this net oscillatory transport was considerably reduced. The longshore current in front of the wall was stronger than that observed on the natural beach. Combined with the increase in suspended sediment, this enhanced longshore current resulted in a longshore sediment transport rate which was an order of magnitude greater in front of the wall than on the natural beach.

ADDITIONAL INDEX WORDS: *Seawall debate, coastal defence, wave reflection, sediment suspension, sediment transport.*

INTRODUCTION

Seawalls are used as a method of coastal protection on many shorelines throughout the world, yet their effects on nearshore sedimentary processes remain surprisingly poorly understood. There is an ongoing debate about whether seawalls alter the local sediment transport regime, and whether this change in sediment transport affects the beach profile (KRAUS, 1988; PILKEY and WRIGHT, 1988; KRAUS and MCDOUGAL, 1996; BASCO *et al.*, 1997). The apparently contradictory observations will begin to make sense only when the processes of wave reflection and sediment transport are properly understood.

For example, laboratory studies of scour troughs have suggested a rhythmic pattern of erosion and accretion extending offshore from a reflective wall. The shape of these bedforms appears to depend on factors such as settling velocity and wave orbital velocity (*e.g.* XIE, 1981; IRIE and NADAOKA 1984; IRIE *et al.*, 1986; FOWLER, 1993; SUMER and FREDSOE, 2000). In the field, scour troughs are most usually observed only at the base of reflective structures, and mostly after storms or hurricanes (*e.g.* SAWARAGI and KAWASAKI, 1960; SEXTON and MOSLOW, 1981; MORTON, 1988). Other effects of seawalls on beaches observed by field experimenters include lowering the beach profile (*e.g.* BIRKEMEIER *et al.*, 1991), slowing beach recovery after storms (*e.g.* KRIEBEL *et al.*, 1986; NAKASHIMA and MOSSA, 1991) and narrowing the beach face (HALL and PILKEY, 1991).

In apparent contradiction are results from some more recent numerical and laboratory models. These have shown that wave reflection may not be a significant contributor to beach profile change or to scour in front of seawalls, and that reflected waves may cause no more sand to be suspended than if there was no seawall present (RAKHA and KAMPHIUS, 1995; MCDOUGAL, *et al.*, 1996). These laboratory results contrast the early laboratory experiments of DORLAND (1940), who found that while waves did not directly cause scour in front of the wall, material was placed in suspension and could then be transported by currents. More recently, TWU and LIAO (1999) used wave flume experiments to investigate the effect of wall slope on scour depth. They found that an increase in steepness of the wall resulted in an increase in reflection coefficient and this lead to an increase in scour depth at the base of the wall.

One approach to understanding the problem is to investigate the sediment suspension and transport processes *in situ,* although this type of study has received little or no attention (KRAUS and MCDOUGAL, 1996). Many process-based field ex-

99053 received 30 May 1999; accepted in revision 21 June 2000.

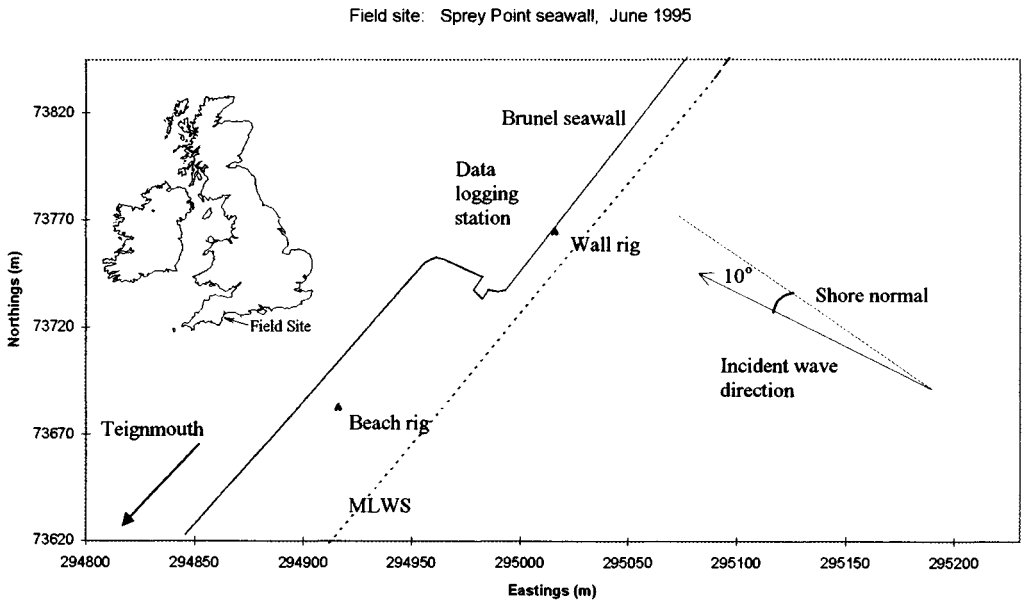

Figure 1. Schematic map of the field site.

periments have taken place on undefended beaches (*e.g.* HUNTLEY and BOWEN, 1975; BEACH and STERNBERG, 1988, 1992; RUSSELL, 1993; DAVIDSON *et al.*, 1993). One of the more frequently used methods is to make high frequency measurements of waves, water velocities and suspended sediment concentrations on the beach. These measurements are leading to a better understanding of sediment transport and beach morphology change on natural beaches, and the analysis techniques can also be applied to the seawall / beach environment.

This paper presents field measurements of sediment transport processes in front of a seawall, with a view to gaining a better understanding of the complex relationship between wave reflection and sediment transport. These measurements are the first of their type in this highly energetic environment.

EXPERIMENTAL DESCRIPTION

Sprey Point at Teignmouth in South Devon, (U.K.) consists of a protruding section of seawall which is fronted by a sandy beach and flanked by beaches on each side. Two instrumented rigs were installed at this field site in June 1995. One rig was mounted on the protruding section of wall (the 'wall rig'), just above the mean water level, and a second rig (the 'beach rig') was sited to the south on a wider section of beach (Figure 1).

The wall at Sprey Point was made of granite blocks, was approximately 7 m high, and the lower half of the wall was sloping at an angle of 53° to the horizontal. The average beach gradient in front of the wall was 0.06 (3.27°). The beach profile was approximately linear, although the beach flattened slightly between the wall and 5 m seaward. No scour trough was observed during the experiment. The beach to the south was of similar slope, having a gradient of 0.07 (3.96°). The grain size of the sand was in the range of medium quartz sand with D_{50} = 0.24 mm. Conditions during the experiment were typical of the site, with wave periods of 4 to 5 seconds and wave heights 0.2 to 0.3 m. Tides were semi-diurnal, with a mean tidal range of 2.9 m. The tidal range was adequate for the rigs to be positioned at low tide, allowing them to measure in the surf and shoaling zones as the tide advected over the instruments.

In previous experiments such as the British Beach And Nearshore Dynamics (B-BAND) programme (RUSSELL *et al.*, 1991) and the Circulation and Sediment Transport Around Banks (CSTAB) project (SIMMONDS *et al.*, 1995), instruments were held in place by rigs buried in the beach. However, during preliminary experiments at this location, rigs of this style failed due to the extremely mobile nature of the sediment bed in front of the wall. It was therefore decided to suspend the instruments from the seawall itself. A rig was constructed of zinc-coated angle iron, and attached to the seawall using bolt and epoxy resin anchors. The complete structure protruded 1.2 m from the wall and was 3.2 m high. The rig was designed to present as little obstruction to the water flow as possible, and visual observations showed that wave reflections were not affected by its presence. No evidence of scour around the base of the rig or by the instruments was found during the experiment. No bedforms were observed at the site at low tide.

Instruments on the wall rig were positioned 1.2 m from the wall, approximately midway between the elevation antinode at the wall and the elevation node just offshore (estimated for wave periods between 3 seconds and 5 seconds). This position in the nodal structure was chosen to obtain the best coherence between elevation and velocity, so that the reflec-

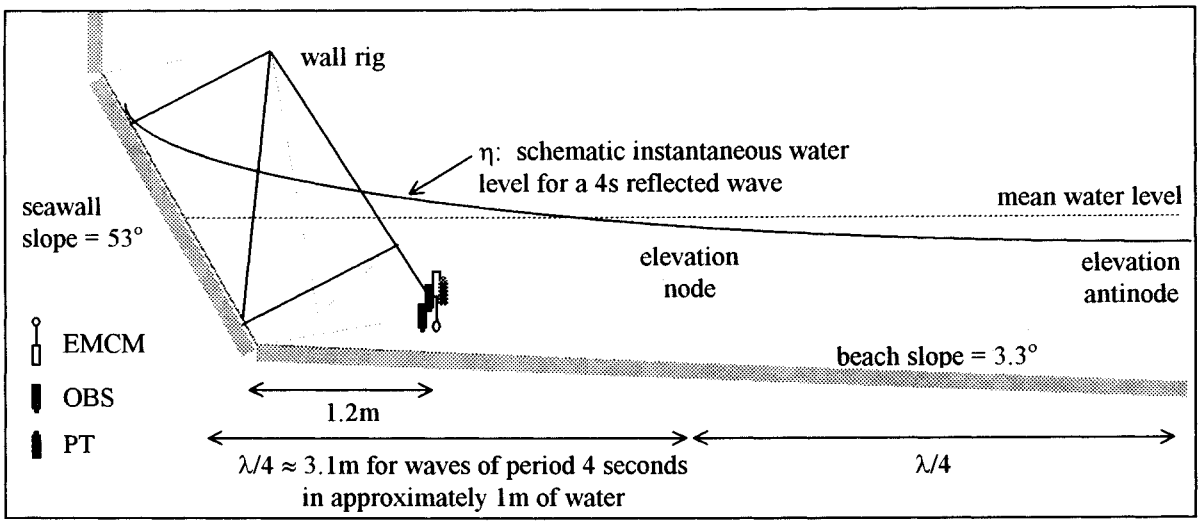

Figure 2. Instrument positions relative to the position of nodes and antinodes.

tion analysis would be as accurate as possible. A schematic of the instrument positions at the wall rig is given in Figure 2. Instrument cables were routed directly to the top of the wall from the instruments.

The beach rig was more conventionally deployed, buried into the beach 135 m south west of the wall rig on a beach contour 0.46 m higher than the wall rig. It was not possible to locate the beach rig on the same contour as the wall rig because the water table remained high as the tide ebbed, making rig deployment on the open beach particularly difficult due to the liquid nature of wet sand. The beach rig was located 15.6 m from the head of the beach. It would therefore not be affected by wave reflections from the wall at the back of the beach unless the water depth over the rig was greater than 1.52 m.

A pressure transducer (PT), a bi-axial electromagnetic current meter (EMCM) and an optical backscatter sensor (OBS) were mounted on each of the two rigs. A second OBS was also mounted on the wall rig directly above the lower OBS. PTs, EMCMs and OBSs were co-located in the vertical / longshore plane in order that they were the same distance from the reflector, beach or wall respectively. EMCMs were carefully aligned so that cross-shore and longshore velocity measurements could be made. Instrument heights above the bed (z) during this run were: Wall: z_{PT} = 0.105m, z_{EMCM} = 0.105m, $z_{OBS\,1}$ = 0.065m, $z_{OBS\,2}$ = 0.165m. Beach: z_{PT} = 0.17m, z_{EMCM} = 0.27m, z_{OBS} = 0.215m.

PTs were pre-calibrated in a deep cylindrical tank. Atmospheric offsets were taken at the start and end of each run. EMCMs were pre-calibrated in a tow-tank. EMCM zero readings were measured *in-situ* using a large container of seawater. Calibrations were applied such that positive velocities imply onshore flow in the cross-shore direction, or northerly flow in the longshore direction. OBSs were calibrated for gain using samples of sediment from the site vigorously stirred in a container of water. Short time averages of OBS output voltage were linearly related to sediment concentration samples taken from the container at the height of the OBS head while stirring. OBS offsets were taken as the background 'zero' level, which showed in the time series as flat sections between sediment suspension events.

Between leaving the instruments and being stored on computer hard disk, the signals were routed along cables, anti-alias filtered and sampled. Data were sampled at 8 Hz in sequential runs of 17.07 minutes. Data were collected for 8 consecutive tides between the 12th and 16th of June, 1995. Data analysed in this paper were collected on the afternoon tide of the 13th June (tide T136PM) when all instruments were functioning, and waves heights were in the region 0.2 m to 0.3 m. Typical time series of wave elevation, cross-shore current and suspended sediment concentrations are shown in Figure 3.

Wave parameters including wave height and water depth for both wall and beach rigs are shown in Figure 4 for this tide. The angle of wave approach was from approximately 10° north of shore normal. Water depths were generally greater at the wall rig, resulting from slightly different cross-shore positions. Wave heights were calculated as $H_s = 4\sigma_{\eta\text{-}g}$ where $\sigma_{\eta\text{-}g}$ is the standard deviation of the surface elevation time series, high pass filtered to obtain the incident wave (gravity band) oscillations. A cut-off frequency of 0.125 Hz was used because a valley in the surface elevation spectrum existed at this frequency. Wave heights were greater at the wall rig due to the proximity of the PT to the elevation antinode. In deeper water, measured RMS velocities were similar at the beach and wall rig, while in shallow water, the measured RMS velocities at the wall rig were generally larger.

The most obvious change in the hydrodynamics which the wall is expected to bring about is an increase in wave reflection. This in turn has been suggested to be responsible for increasing sediment suspension, and sediment that is suspended can easily be transported. The research presented in

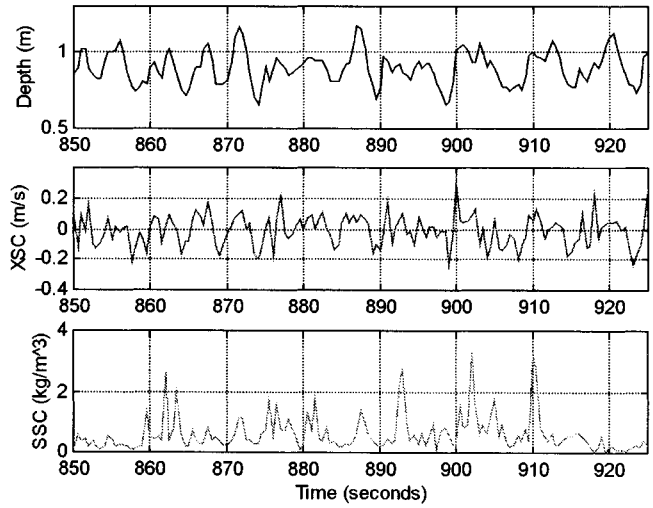

Figure 3. Example time series of surface elevation (Depth), cross-shore velocity (XSC) and suspended sediment concentration (SSC) at the seawall.

the next sections follows this theme for investigation and analysis. Frequency dependent reflection coefficients have been obtained from elevation and velocity traces at both wall and beach rigs. Suspended sediment concentrations in front of the wall have been compared to those on the beach, and sediment transport has been determined using both time domain and frequency domain analysis of the velocity and sediment time series. Results for both wall and beach cases are compared and discussed in the following sections.

WAVE REFLECTION ANALYSIS

Wave reflection coefficients can be calculated from the time series of pressure and velocity using methods in the time and frequency domains.

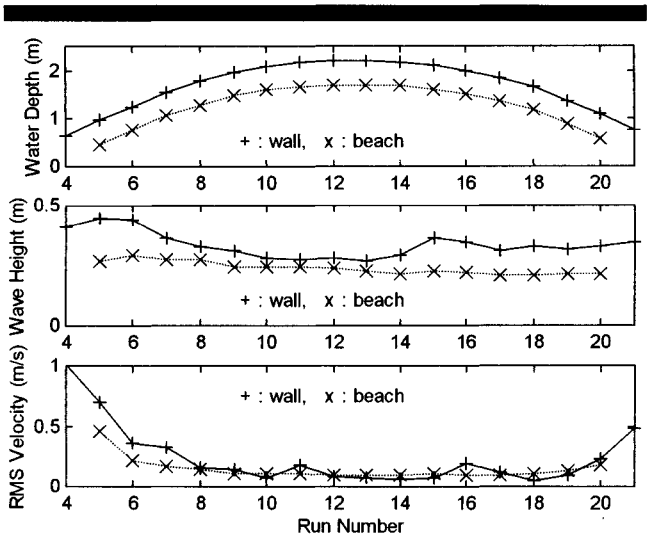

Figure 4. Simultaneous water depths, wave heights and RMS velocities measured at the beach and wall rigs during the PM tide of 13th June, 1995. Runs were of length 17 mins, and were sequential.

Time Domain Analysis

GUZA *et al.* (1984) give equations for determining the incoming and outgoing surface elevation time series of shallow waves on a beach directly from the measured surface elevation and velocity time series ($\eta(t)$ and u(t) respectively, with u +ve onshore):

$$\eta_{in}(t) = \left[\eta(t) + \sqrt{\frac{h}{g}}u(t)\right] \Big/ 2$$

$$\eta_{out}(t) = \left[\eta(t) - \sqrt{\frac{h}{g}}u(t)\right] \Big/ 2 \qquad (1)$$

Incident and reflected wave spectra can be calculated directly from these time series.

If $S_{ii}(f)$ is the spectrum of the incoming wave time series and $S_{oo}(f)$ is the spectrum of the outgoing wave time series, the frequency dependent reflection coefficient R(f) is given by:

$$R(f) = \sqrt{\frac{S_{ii}(f)}{S_{oo}(f)}} \qquad (2)$$

This method is simple to apply to data from co-located sensors, but it is only applicable in shallow water. By carrying out a similar analysis in the frequency domain it is possible to eliminate this problem, as the full dispersion equation can be solved for each frequency.

Frequency Domain Method

HUNTLEY *et al.* (1995) show that the reflection coefficient can be re-arranged in the frequency domain to give:

$$R^2(f) = \frac{1 + G^2(f) - 2G(f)\cos\theta_{\eta u}(f)}{1 + G^2(f) + 2G(f)\cos\theta_{\eta u}(f)} \qquad (3)$$

where $\theta_{\eta u}(f)$ is the phase spectrum between elevation and velocity, the gain G(f) is given by:

$$G(f) = \sqrt{\frac{S_{\eta\eta}(f)}{S_{uu}(f)}} \qquad (4)$$

$S_{\eta\eta}(f)$ is the spectrum of elevation, and $S_{uu}(f)$ is the spectrum of the elevation estimated from the velocity using linear theory. This method can be used in both shallow and intermediate water.

HUNTLEY *et al.* (1995) investigated the effect of noise on the time and frequency domain methods. They found that in the presence of noise, Guza's method consistently overestimated the reflection coefficient while the frequency domain method underestimated it.

Principal Component Analysis

A third technique, the principal component analysis (PCA hereafter), has been suggested to be better at reducing the effects of noise in the signal than the previous two methods (TATAVARTI *et al.*, 1988 and TATAVARTI, 1989). In this method, eigenvectors are used to extract the well correlated parts of the elevation and velocity signals.

The validity of this approach has been tested on simulated data and field measurements and compared against the other two methods by HUNTLEY *et al.* (1999) and found to be essentially bias free, except for very low values of coherence, and for reflection coefficients very close to one. It thus appears that for the case of waves reflecting from natural beaches the PCA method provides the most useful method of wave reflection analysis, however for the case of waves interacting with a seawall, the reflection coefficient tends to unity at both incident and infragravity frequencies, and the method may not be as applicable. In order that errors brought about by any one of the above methods would be high-lighted, all three methods were applied to data gathered in this experiment, and the results compared.

A bulk reflection coefficient for the gravity band (or any other frequency band of interest) can be obtained from any of the three frequency domain methods above by averaging the reflection coefficient estimates for frequencies where the in/out coherence is greater than the 95% confidence level on the coherence. This is given by:

$$r = \frac{1}{n} \sum_{\text{freq band}} R_c(f) \qquad (5)$$

where r is the bulk reflection coefficient, in this case averaged over the gravity band, $R_c(f)$ are the reflection coefficient estimates at frequencies (f) which have coherent in/out time series, and n is the number of these estimates. Calculation of the gravity band reflection coefficient for each run shows how it evolves through the tide.

WAVE REFLECTION RESULTS

Incoming and outgoing wave spectra were calculated for both beach and wall cases. The spectra in Figure 5a show incoming wave energy spectra (solid line) and outgoing wave energy spectra (dashed line) at the beach when the water depth at the instrument was 1.4 m (well outside the surf zone). Gravity band energy ($0.125 < f < 0.36$ Hz) incident on the beach is clearly dissipated and not reflected. Energy at lower frequencies ($0.04 < f < 0.125$ Hz) is present as incident and reflected waves. Coherence between the elevation and velocity (P/U coherence in 5d) is high in the incident wave band, and this is to be expected in the case of the progressive waves. The coherence between the incoming and outgoing waves calculated from the elevation and velocity time series also has peaks of high coherence in the incident wave band, even though there is little energy in the outgoing time series (5b).

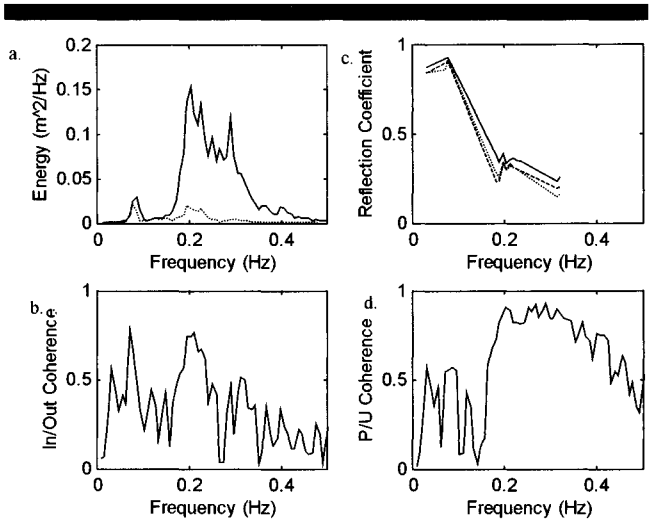

Figure 5. Frequency dependent wave reflection at the beach. a) Incoming (solid line) and outgoing (dashed line) wave spectra calculated using the time domain method. b) Coherence between calculated incoming and outgoing time series. c) Frequency dependent reflection coefficient calculated using time domain (solid line), frequency domain (dashed line) and principal component analysis (dotted line) methods (plotted for in/out coherence > 0.5). d) Coherence between elevation (denoted 'P') and velocity. Water depth is 1.4 m (run 9).

The frequency dependent wave reflection coefficient is presented in Figure 5c. The results of the time domain method, (solid line), the frequency domain method (dashed) and the PCA method (dotted) are shown. Results are only presented for frequencies which have values of coherence between incoming and outgoing waves greater than 0.5 to minimise the bias on the reflection coefficient estimate (HUNTLEY *et al.*, 1999). At incident wave frequencies and frequencies lower than the incident waves, the time domain method clearly gives estimates of reflection coefficient which are slightly larger than the frequency domain methods. However the bias is small, and the overall shape of the graphs is very similar. The general shape of the frequency dependent reflection coefficient shown by all three methods is very much as expected—high reflection coefficients for low frequency waves indicate that they are reflected rather than dissipated by the beach while incident waves are almost completely dissipated. Results similar to this were consistently found for measurements taken outside the surf zone of the natural beach.

An identical analysis was carried out on data collected at the wall at the same time in a similar water depth (1.3 m). The results of this analysis are presented in Figure 6. In this case the incoming and outgoing wave energies are of similar magnitudes (6a) at all frequencies. There are slight differences however through frequency. While at low frequency reflection is almost complete, at incident wave frequency some

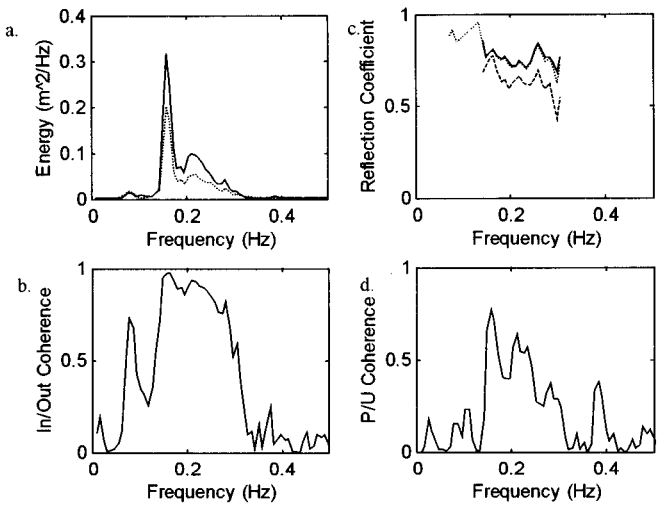

Figure 6. Frequency dependent wave reflection at the wall. a) Incoming (solid line) and outgoing (dashed line) wave spectra calculated using the time domain method. b) Coherence between calculated incoming and outgoing time series. c) Frequency dependent reflection coefficient calculated using time domain (solid line), frequency domain (dashed line) and principal component analysis (dotted line) methods (plotted for in/out coherence > 0.5). d) Coherence between elevation and velocity. Water depth is 1.3 m (run 6).

dissipation of energy has occurred. The coherence between the elevation and velocity is high within the incident wave band, and is lower in other frequencies (6d). Even in the incident wave band the elevation-velocity coherence is not as high as for the beach case, and this is likely to be a result of the proximity of the instruments to the elevation antinode at the wall. The reflection coefficients at the wall are larger than at the beach, as expected. The time domain method and PCA method provide remarkably similar estimates for the reflection coefficient in this case, while the frequency domain method provides a lower estimate.

The evolution of the gravity band averaged bulk reflection coefficient through the tide for wall and beach cases is shown in Figure 7. Reflection coefficients at the wall are much larger than at the beach throughout the tide. At the wall, reflection coefficients generally increased during the flood tide as the water gets deeper, and there is less dissipation. During the ebb, the reflection coefficient stays high in this case. This may be because of a reduction in wave height during the tide (see Figure 4), which would give rise to less dissipation. Reflection coefficients at the beach are initially <0.2, although are they are larger between runs 9 and 17 ($r \cong 0.4$), coinciding with a small amount of reflection from the wall at the back of the 'natural' beach, 15.6 m shoreward.

Generally, deeper water and smaller wave heights at the wall gives rise to less dissipation and this results in a higher reflection coefficient. While the increase in depth allows the reflection coefficient to increase, as there is less dissipation, there is less interaction between the waves and the bed, and larger water depths are therefore likely to lead to less sediment suspension and transport. The link between reflection

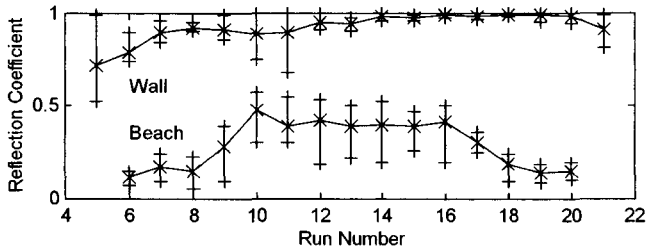

Figure 7. Reflection coefficients (averaged over incident wave band) for wall and beach cases. Vertical bars indicate maximum and minimum values in incident wave frequency band.

coefficient, water depth and sediment concentration is investigated in the next section.

SEDIMENT SUSPENSION AND TRANSPORT ANALYSIS

Mean Sediment Concentrations

The vertical profile of mean suspended sediment concentration was given by NIELSEN (1984) as:

$$\bar{c}(z) = c_o e^{z/l_s} \quad (6)$$

where $\bar{c}(z)$ is the mean sediment concentration at some height z above the bed, c_o is the reference concentration at the bed, and l_s is a vertical length scale representing the balance between vertical diffusivity and settling. If concentrations at two points in the vertical profile are known, it is possible to solve for c_o and l_s, and predict the mean sediment concentration at any other height. In this experiment, this technique is used to compare measurements of mean suspended sediment concentration at the beach (at z = 0.215 m) with those at the wall (measured at z = 0.065 m and 0.165 m, and predicted for z = 0.215 m). Investigation using this technique showed the concentration predicted at 0.215 m was, on average of 79% of the concentration measured at 0.165 m. The height difference was therefore considered important when quantifying the difference between mean sediment concentrations at the wall and the beach, but less important for the process interpretation of mean and oscillatory sediment fluxes.

Sediment transport

Sediment transport is routinely split into mean and oscillatory components after JAFFE *et al.* (1984). The net transport at the height of the instruments can be expressed in terms of the flux due to the mean velocitiy and concentration ($\bar{u}$ and $\bar{c}$ respectively), plus the transport due to the flux coupling between oscillatory components (u'c'):

$$\langle UC \rangle = \bar{u}\bar{c} + \langle u'c' \rangle \quad (7)$$

where $\langle\ \rangle$ denotes time average. This analysis allows the sediment transport by mean flows (due to cross-shore and longshore currents) to be separated from the oscillatory component that results from the regular suspension of sediment during one phase of the wave cycle. The oscillatory compo-

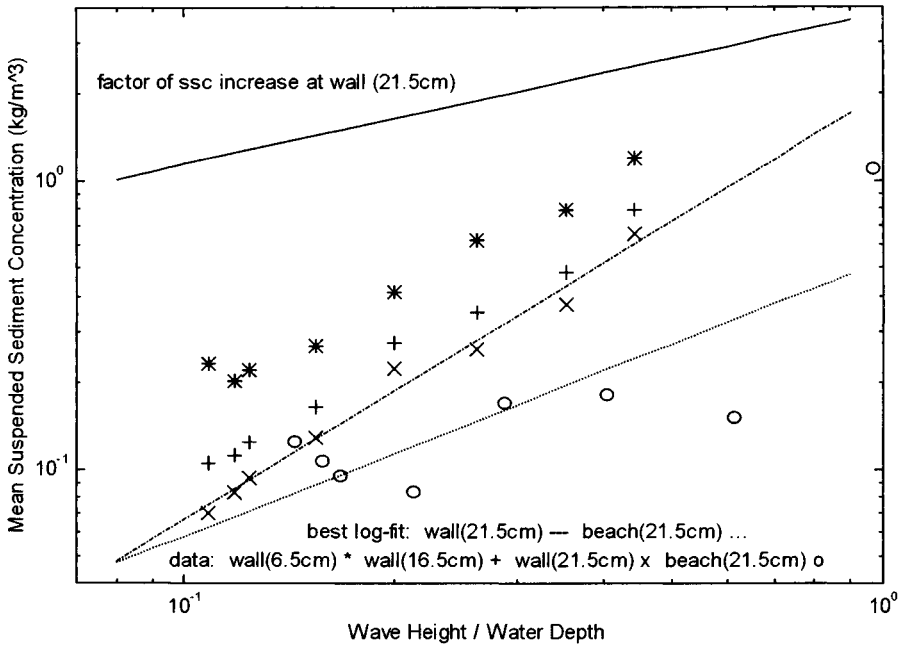

Figure 8. Mean suspended sediment concentrations measured at the wall at 6.5 and 16.5 cm, and predicted at 21.5 cm, compared with measurements at the beach at 21.5 cm.

nent can be further decomposed in the frequency domain using the co-spectrum to identify the dominant frequencies of sediment transport (HUNTLEY and HANES, 1987).

SEDIMENT SUSPENSION AND TRANSPORT RESULTS

Mean Sediment Concentrations

Both DORLAND (1940) and SILVESTER (1977) suggested that the reflection of the incident wave energy over a beach provides more energy for sediment suspension. The time series of sediment suspension at the wall and beach initially indicated that more sediment was being suspended in front of the wall than on the natural beach during similar incident wave conditions. The suspended sediment concentrations increased in shallower water, and also with increasing wave height. Mean sediment concentrations calculated for the wall at 0.215 m were compared with those measured at the beach at 0.215 m for different ratios of incident wave height to mean water depth (H/h) for the flood tide of T136PM (Figure 8).

Mean concentrations in front of the wall were found to be up to three times larger than those on the beach for H/h < 0.7. The maximum difference occurred for the largest values of wave height over water depth. In deep water and with smaller waves (i.e. smaller H/h), the difference was less pronounced. The difference was also less pronounced on the ebb tide, when wave heights were smaller. The best fit equation for the ratio of sediment concentration at the wall to sediment concentration at the beach for equal H/h, and for the same height above the bed, was given by:

$$\frac{\bar{c}_{wall}}{\bar{c}_{beach}} = 3.8\left(\frac{H}{h}\right)^{0.52} \quad (8)$$

These results represent conditions outside the surf-zone. In the band of relative wave height given by $0.076 < H/h < 0.78$, equation 8 gives a factorial increase of suspended sediment concentration of $1 < \bar{c}_{wall}/\bar{c}_{beach} < 3.3$.

Suspension of Sediment

Both in front of reflective structures and on natural beaches, hydrodynamic forcing is responsible for suspending and then transporting sediment. The nature of the water movement in front of the seawall was found to be rather different to that measured on the adjacent natural beach, and the resulting sediment suspension events were often rather different in appearance. In front of a wall with a high reflection coefficient, the velocity generally leads the elevation. The exact phase angle depends on the reflection coefficient. It is plausible that as the velocity increases as a wave passes any point, so the shear increases, until sediment is suspended (BAGNOLD, 1946). Sediment suspension thereby occurs in phase with the velocity maximum, and is 'shear driven'. (see Figure 9a, event A).

To break down the interaction of incoming and outgoing waves, a data simulation was employed using an incident and reflected solitary wave (Figure 9b). An onshore travelling wave suspends sediment at the same time as its velocity maximum (Figure 9b, event A), and reflects at the wall. For the purposes of this example, a reflection coefficient of 0.9 was used. The suspended sediment concentration was assumed to be an instantaneous function of the velocity magnitude cubed.

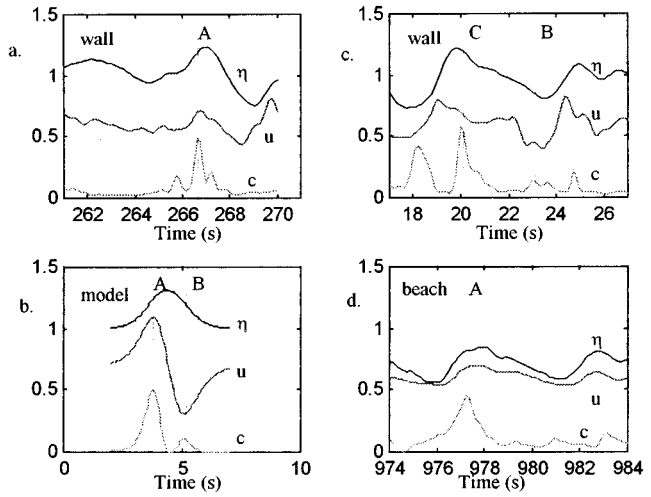

Figure 9. Time series examples showing elevation (η), velocity (u) and sediment suspension events (c) a) measured at the wall: in phase with velocity, b) modelled at the wall: in phase with velocity c) measured at the wall: out of phase with velocity d) measured at the beach: in phase with velocity. Units of η, u and c are m, m/s and kg/m^3 respectively. Velocity values are offset of +0.6 m/s for clarity. Suspended sediment concentrations are scaled to one tenth their measured values. Three types of suspension event are highlighted. A: sediment concentration peaks in phase with onshore velocity, B: sediment concentration peaks with reflected wave, C: sediment concentration peaks at flow reversal.

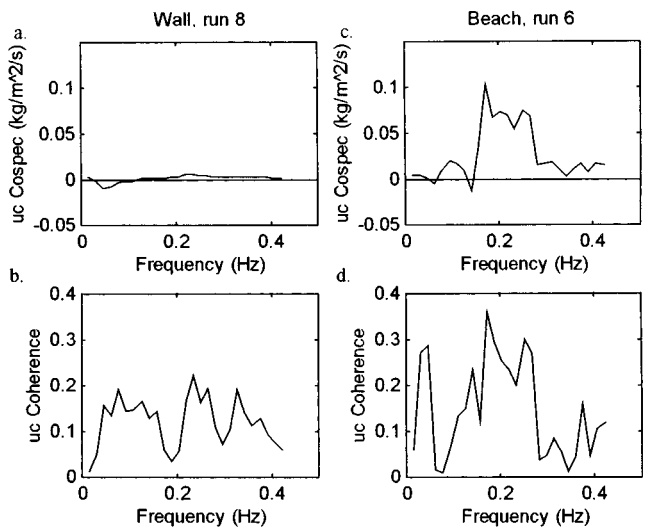

Figure 10. Co-spectra between velocity and suspended sediment concentration: a) at the wall, c) at the beach. Coherence between suspended sediment and the velocity is given for the wall and beach cases by b) and d) respectively.

On passing the instruments on its way seaward, the reflected wave also suspends sediment (Figure 9b, event B). The reflected wave suspension event is smaller than the incident wave suspension event because the reflection coefficient is less than unity, and because the near-bed mean flow was onshore (as observed at the instruments and included in the simulation). This weights the 'shear driven' sediment suspension to favour the onshore phase of the wave. The net oscillatory sediment transport was therefore onshore in the simulation, although this onshore transport of sediment was reduced by the presence of a reflector. The offshore travelling wave shows in the velocity time series as an offshore flow, at the same time as a drop in elevation, (9b), (depending on the distance to the reflector). An example of a small sediment suspension event associated with an offshore directed flow in the reflective environment is visible in Figure 9c, event B.

Sediment suspension events have also been observed during acceleration phases of the wave (HANES and HUNTLEY, 1986). During this time the velocity is zero, and this type of event has also been termed a 'flow reversal event', where the boundary layer loses its identity while the velocity is zero, and turbulence which was constrained by the boundary layer brings sediment up into the water column (MURRAY, 1992; FOSTER *et al.*, 1994). Suspension events in front of the wall were also regularly observed to occur during such flow reversals (Figure 9c, event C), although interestingly they often start while the velocity is maximum. The phase of the wave at which the measured sediment concentration reaches its maximum determines both the direction and magnitude of the transport. The phase of suspension and the resulting direction of sediment transport can also be modified by bedforms (*e.g.* wave ripples), although measurements of bedforms were not possible during this experiment.

On the natural beach, the maximum of a suspension event most often occurred at the phase of the wave when the velocity was onshore, although in many cases it would be growing while the fluid was accelerating (see Figure 9d, event A). This process clearly results in a net onshore sediment transport, as sediment is effectively 'pumped' shoreward. Events at the seawall such as that in (9a) also result in onshore transport. However, a significant number of events at the wall occurred during flow deceleration (as in Figure 9c, event C), and during offshore directed flows (as in Figure 9c, event B) to reduce the net onshore transport of sediment by waves considerably.

Wave Driven Sediment Transport

Where oscillations of sediment and velocity are regularly in phase, this will lead to a net transport, indicated by the flux coupling $\langle u'c' \rangle$ and the area under the co-spectrum (HUNTLEY and HANES, 1987). Where suspension events happen on both onshore and offshore phases of the wave, or the suspension event is in quadrature with the velocity, the net oscillatory transport is reduced. Figure 10 shows co-spectra between suspension and velocity and associated coherences calculated from 17 minutes of data for the beach and wall cases. At the beach, the net oscillatory transport is clearly onshore (positive values of co-spectrum), and is dominated by motion at the same frequency as the incident waves. At the wall, there is only a very small net oscillatory transport compared to at the beach rig, despite larger amounts of sediment being suspended at the wall in similar incident wave conditions. This results from the different phases of suspension,

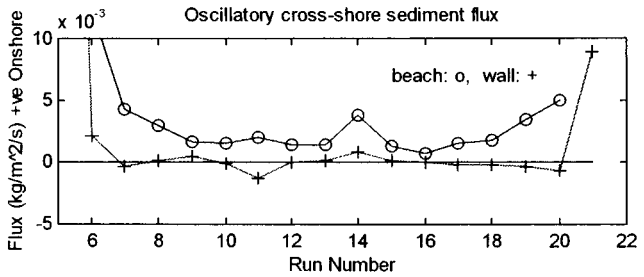

Figure 11. Oscillatory cross-shore fluxes ($\langle u'c' \rangle$) at wall and beach rigs.

and the balance in onshore transport by incoming waves and offshore transport by outgoing waves at the wall rig.

The oscillatory component of the cross-shore sediment flux ($\langle u'c' \rangle$) was calculated for all runs in beach and wall cases (Figure 11). At the beach rig, the cross-shore sediment transport by waves was onshore throughout the tide, and increased in shallow water. Onshore oscillatory sediment transport was much reduced at the wall rig throughout the tide compared to the beach rig, consistent with the co-spectral results above.

Cross-shore Mean Velocities and Fluxes

Onshore mean flows of 0.01 to 0.11 m/s were recorded at the wall (Figure 12). The gradual decrease in mean onshore velocity is a result of the gradual decrease in wave activity throughout the tide. The mean component of sediment transport ($\bar{u}\bar{c}$) at the wall was onshore, and decreased dramatically as the water deepened to high water and as the wave activity decreased (Figure 13). $\bar{u}\bar{c}$ was large compared to the flux coupling ($u'c'$). This is because although waves did suspend large amounts of sediment at the wall (giving large $\bar{c}$, and hence large $\bar{u}\bar{c}$) , the suspension events occurred at phases of the wave such that there was little net oscillatory sediment transport.

Cross-shore currents at the beach rig were found to be offshore (Figure 12), consistent with the solution for the profile of mass transport within a progressive wave by LONGUET HIGGINS (1953). The mean sediment transport past the beach rig followed the mean current, and was therefore directed offshore at the height of the instrument (Figure 13).

However, the depth averaged net sediment transport due to the mean currents at the beach rig may in fact be onshore, as the boundary layer transport would be in the direction of wave advance. Other workers have found mean transports near the bed to be onshore outside the surf zone (*c.f.* RUSSELL *et al.*, 1991), and as the values lie inside the 10% error bar, the observed offshore mean current past the beach rig is not conclusive.

Longshore Mean Velocities and Fluxes.

A strong longshore current was observed to flow along the wall to the south (Figure 12). This current was significantly larger than on the adjacent natural beach. The mean longshore sediment flux at the wall is in the same direction as

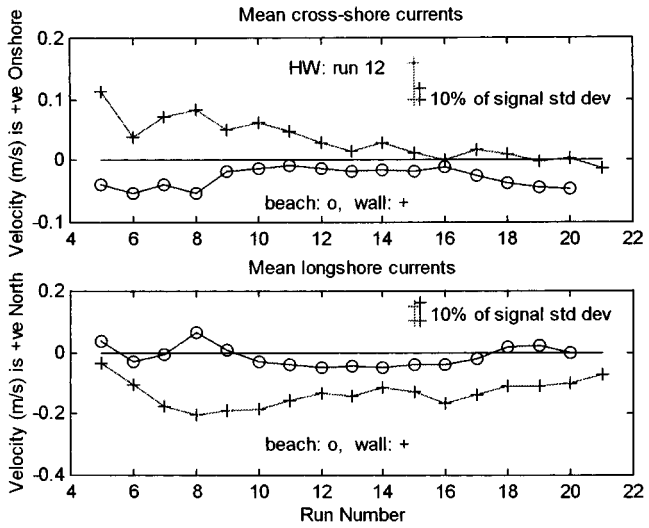

Figure 12. Mean velocities ($\bar{u}$ and $\bar{v}$) at wall and beach rigs.

the mean flow, and is considerably greater than that observed at the beach (Figure 13). Longshore sediment transport in front of the seawall was therefore observed to be enhanced by both an increased longshore current, *and* an increase in suspended sediment concentration at the wall, driven by wave reflection.

DISCUSSION

The results of this field experiment have shown that the seawall can significantly affect the amount of material in suspension, and can also affect its mode of transport. Generally, the measurements agree with the laboratory observations of DORLAND (1940) and the suggestions made by SILVESTER (1977). The suspension of sediment was increased in front of

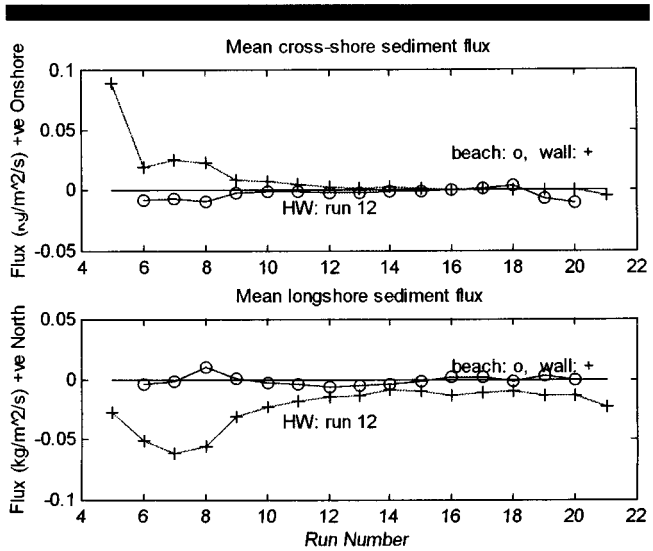

Figure 13. Mean sediment fluxes ($\bar{u}\bar{c}$ and $\bar{v}\bar{c}$) at wall and beach rigs.

the wall by the wave reflections, and this sediment was then transported by mean currents. In particular, the increase in suspended sediment contributed to an enhanced longshore sediment flux. Further to the original observations, wave reflections were found to affect the oscillatory sediment transport. The reflections significantly reduced the net onshore transport of sediment by waves, a process that would slow the recovery of the beach. The observation that the presence of a seawall can slow the recovery of the beach has also been made by KRIEBEL (1987), SAYRE (1987) and NAKASHIMA and MOSSA (1991).

Mean cross-shore currents were found to agree generally with the results of LONGUET HIGGINS (1953), however there were not sufficient measurements to determine the extent or strength of any circulation cells. Neither scour nor rhythmic bars were observed in front of the wall, such as those suggested by XIE (1981), although waves were small and conditions were therefore accretionary.

The increased longshore current in front of the wall combined with the enhanced suspended sediment concentration to create a strong longshore sediment flux in front of the wall. The mechanism driving the longshore current is not fully understood. It may be a result of the constriction to the longshore flow offered by the Sprey Point wall, which could accelerate the flow past it, or it may be a result of a slightly oblique wave reflection (incident waves approached at approximately 10° north of shore normal). Further research into this process is required, as such a longshore jet may well exceed the threshold for sediment suspension, and give rise to localised scour.

One limitation of the experiment carried out, is that measurements were only made at one distance from the wall. Given the range of wave periods within the incident band of the spectrum, the instruments were positioned within some form of moving nodal structure. For analysis of the structure of mean flows in the nodal structure, data from one point is obviously deficient. However, for wave driven processes such as incident wave frequency sediment suspension, it could be argued that the results would hold for a large proportion of the nodal structure. Local suspension of sediment can be assumed, because orbital excursions are not large enough in the region of the instruments to advect sediment from the node or antinode to the instruments. The reflection of waves at the wall in shallow water gives rise to separate incoming and outgoing waves, which interact as they pass each other. These separate waves each affect the sediment. Suspension of sediment is clearly a result of the total velocity. However, in shallow water, where waves are of higher order than linear or cnoidal, the outgoing waves may act on the sediment reasonably independently of the incoming waves. The data in this experiment shows incoming and outgoing waves both driving suspension events (as in the data simulation, Figure 9). At different cross-shore positions in the nodal structure, it would be reasonable to expect that the time lag between peaks in suspension would depend on the time taken for the wave to pass the instruments, be reflected at the wall, and return to the instruments. The total suspended sediment concentration would therefore not depend particularly on the position in the nodal structure, but on the magnitude of the velocities associated with the shoaling (incident) and reflected waves. The extra suspension given as a result of the outgoing waves could therefore directly lead to an increase in mean sediment suspension.

The data are also limited by being point measurements, each made from one height above the bed. The heights of the instruments at the wall and beach rigs were also slightly different. For mean sediment concentrations, it was possible to quantify the vertical shear in the suspended sediment concentration at the wall using the measurements from 6.5 and 16.5 cm, and applying NIELSEN's (1984) equation. Using this, a prediction for the concentration at 21.5 cm was possible, to compare with the measurements on the beach at 21.5 cm. The vertical shear for the height difference between 16.5 cm and 21.5 cm was small however, with an average relationship between the two of $\bar{c}_{21.5} = 0.79\ \bar{c}_{16.5}$.

The phase of suspension is important in indicating the direction of the oscillatory sediment transport. For the instruments to be representative of the entire profile, the suspension of sediment measured at the instruments must be in phase with the sediment concentrations in the rest of the water column. Cross-correlation between the lower and upper OBSs on the wall rig showed no time lag between the two sensors. The phase of suspension was therefore assumed to be constant through depth, and the measurements at the instrument heights considered representative of the profile.

Current measurements were also made at slightly different heights above the bed (27 cm at the beach, and 10.5 cm at the wall). For shallow water oscillatory flows, the incident wave boundary layer extends to within 2–3 cm of the bed, and the velocity shear in the vertical is very small. The phase of the oscillatory velocity through the vertical is close to constant, and the measurements made at the two heights are therefore comparable. Measurements made at the heights of the instruments are therefore also representative of the entire profile for the oscillatory component.

For mean tidal flows in which the current direction does not reverse in the water column, SOULSBY's (1990) $1/7^{th}$ law can be applied, to give the ratio between velocities at different heights above the bed ($u_1/u_2 = (z_1/z_2)^{1/7}$) . When applied to the instrument heights in this experiment, the current at 27.5 cm (beach rig) would be 14% larger than the current at 10.5 cm (wall rig) if the instruments were subjected to the same flow. This difference is small, and close to the 10% error bar generally associated with EMCMs. This is most applicable to the longshore current and flux measurements. Despite being measured lower down in the water column (and therefore possibly underestimated), longshore currents at the wall rig were considerably larger than at the beach rig. The exact vertical structure of the longshore current at the beach and wall rig was not measured, and flux measurements are therefore presented at the height of the instruments. Sediment flux values calculated at the wall are therefore slightly overestimated by the OBS measurement height, and slightly reduced by the current measurement height.

The vertical height difference calculation of SOULSBY (1990) does not apply to the cross-shore case however, as the structure of the mean cross-shore current in both wall and beach cases is complex. Vertical circulations of water can ex-

ist in front of a reflector (i.e. at the wall), and at the beach the direction of the net drift in a progressive wave depends on the height above the bed. The cross-shore mean fluxes can therefore only indicate the directions at the heights of the EMCMs. All these limitations can only be overcome by having more instruments than were available during this experiment.

One difference between the rigs was that the beach rig was on a slightly higher contour than the wall rig. The wall rig was located at MWL, while the beach rig was located at MWL+0.46 m. However, the beach slope in front of the wall was similar to the natural beach, incident waves were identical and the sediment grain size was the same at both sites. The beach rig position was therefore considered a valid control site. Wave heights remained reasonably constant through the tide of data presented in this paper, although they did drop slightly towards the end of the tide. The main difference between the two sites was therefore the water depth. For process interpretation of currents and fluxes, their evolution through the tide was considered the most informative. For quantitative comparison, the mean sediment concentrations were normalised using the wave height / water depth ratio.

Conditions were generally accretionary at the beach, although the accumulation of sediment took place shoreward of the beach rig (visual observation) and it was not possible to quantify this immediately before and after the T136PM tide. Measurements at the start and end of the 5 days for which the experiment was carried out showed an increase in level of 40 cm at the back of the natural beach, while at the wall there was only 4 cm accretion. Wave heights were similar or smaller to those presented in this paper throughout that time. Therefore, sediment that was measured moving onshore at the beach rig gave rise to an increase in beach level. At the wall rig however, the onshore transport of sediment was inhibited. A small amount of accretion at the beach rig (5 mm) was noted between the start and the end of tide T136PM. This would have negligible effect on the process measurements made. No accretion was measured at the wall rig between the start and end of the measurements discussed in the paper.

To summarise, a single array of instruments in front of a seawall revealed that an increase in the reflection coefficient resulting from the wall can increase sediment suspension by up to a factor of three. Further field measurements with a denser array of instruments are recommended to examine the cross-shore distribution of this increase, and to identify the wave conditions under which beaches in front of seawalls are most vulnerable to erosion.

These results do have implications for future coastal engineering works. The research is not intended to show seawalls as 'bad' or 'good', as their use depends on a large number of physical, social and economic factors. In terms of the dynamics, both wave reflection and wave dissipation over the bed in shallow water result in extra suspension. Where coastal structures are required to hold the coastal line, it would therefore appear sensible to make them as internally dissipative as possible (e.g. rubble mound), thereby reducing both reflection over the bed and dissipation over it. In some circumstances, vertical seawalls are deemed necessary, and careful monitoring of sand levels would be appropriate in these cases.

CONCLUSIONS

A field experiment was carried out at Teignmouth, in South Devon, U.K. to examine the effects of seawalls on the beach. Incident wave reflection coefficients at the natural beach were small ($R \cong 0.25$ for $f \cong 0.2$ Hz), indicating that incident wave energy was mostly dissipated. Wave reflection coefficients at the wall were typically in the region $0.7 < R < 1.0$. Mean onshore flows in the range $0 < u < 0.12$ m/s were recorded 1.2 m away from the wall, approximately midway between the elevation node at $\lambda/4$ and the wall antinode, in the lower half of the water column. Longshore currents were considerably larger in front of the wall than those on the adjacent natural beach. Typical values were $0.05 < v_{wall} < 0.2$ m/s, compared with $0 < v_{beach} < 0.05$ m/s. Mean sediment concentrations in front of the wall were up to three times larger than on the adjacent natural beach, and increased with increasing wave height and decreasing water depths. Sediment transport by waves was onshore at both wall and beach, however it was much reduced at the wall due to the phase of suspension. The mean longshore sediment flux was considerably enhanced by the presence of the seawall. Typical longshore sediment flux values were in the range $0.01 < \bar{v}\bar{c}_{wall} < 0.06$ kg/m^2/s and $0.00 < \bar{v}\bar{c}_{beach} < 0.01$ kg/m^2/s.

The results confirm that seawalls can have a significant effect on the transport of beach material. Wave reflections, mean flows, mean sediment concentrations and the magnitudes of different modes of sediment transport were all found to be affected by the presence of the wall. Further experiments are recommended to examine the wider spatial and temporal distribution of these parameters in front of seawalls.

ACKNOWLEDGEMENTS

The authors would like to thank Mr Peter Ganderton from the University of Plymouth for his technical assistance during the fieldwork phase of this research.

LITERATURE CITED

BAGNOLD, R.A., 1946. Motion of waves in shallow water; interactions between waves and sand bottom. *Proceedings of the Royal Society,* London, series A, 187, 1–15.

BASCO, D.R.; BELLOMO, D.A.; HAZELTON, J.M., and JONES, B.N., 1997. The influence of seawalls on subaerial beach volumes with receeding shorelines. *Coastal Engineering,* 30, 203–233.

BEACH, R.A. and STERNBERG, R.W., 1988. Suspended sediment transport in the surf zone: response to cross- shore infragravity motion. *Marine Geology,* 80, 61–79.

BEACH, R.A. and STERNBERG, R.W., 1992. Suspended sediment transport in the surf zone: Response to incident wave and longshore current interaction. *Marine Geology,* 108, 275–294.

BIRKEMEIER, W.A.; BICHNER, E.W.; SCARBOROUGH, B.L.; MCCARTHY, M.A., and EISER, W.C., 1991. Nearshore profile response caused by Hurricane Hugo. *In:* FINKL, C.W. and PILKEY, O.H. (Ed.s), Impacts of Hurricane Hugo. *Journal of Coastal Research,* Special Issue No. 8, 113–127.

DAVIDSON, M.A.; RUSSELL, P.E.; HUNTLEY, D.A., and HARDISTY, J.,

1993. Tidal asymmetry in suspended sand transport on a macrotidal intermediate beach. *Marine Geology,* 110, 333–353.

DORLAND, G.M., 1940. *Equilibrium Sand Slopes in Front of Seawalls.* Unpublished M.S. Thesis, Department of Civil Engineering, University of California, Berkely, California, 43p.

FOSTER, D.L.; HOLMAN, R.A., and BEACH, R.A., 1994. Sediment suspension events and shear instabilities in the bottom boundary layer. *Proceedings of Coastal Dynamics '94,* 712–726.

FOWLER, J., 1993. Coastal scour problems and methods for prediction of maximum scour. *Technical Report CERC-93-8,* U.S. Army Engineer Waterways Experiment Station, Coastal Engineering Research Center, Vicksburg, Miss.

GUZA, R.T.; THORNTON, E.B., and HOLMAN, R.A., 1984. Swash on steep and shallow beaches. *Proceedings of 19th Conference on Coastal Engineering,* American Society of Civil Engineers, 708–723.

HALL, M.J. and PILKEY, O.H., 1991. Effects of hard stabilization on dry beach width for New Jersey. *Journal of Coastal Research* 7(3), 771–785.

HANES, D.M. and HUNTLEY, D.A., 1986. Continuous measurements of suspended sand concentration in a wave dominated nearshore environment. *Continental Shelf Research* 6, 585–596.

HUNTLEY, D.A. and BOWEN, A.J., 1975. Comparison of the hydrodynamics of steep and shallow beaches. *In:* HAILS, J. and CARR, A. (Eds.), *Nearshore Sediment Dynamics and Sedimentation,* John Wiley and Sons Ltd., London, pp 69–109.

HUNTLEY, D.A. and HANES, D.M., 1987. Direct measurement of suspended sediment transport. *Proceedings of Coastal Sediments '87,* American Society of Civil Engineers, 723–737.

HUNTLEY, D.A.; SIMMONDS, D., and DAVIDSON, M.A., 1995. Estimation of frequency-dependent reflection coefficients using current and elevation sensors. *Proceedings of Coastal Dynamics '95,* 57–68.

HUNTLEY, D.A.; SIMMONDS, D., and TATAVARTI, R., 1999. Use of collocated sensors to measure coastal wave reflection. *Journal of Waterway, Port, Coastal and Ocean Engineering,* 125(1), 46–52.

IRIE, I. and NADAOKA, K., 1984. Laboratory reproduction of seabed scour in front of breakwaters. *Proceedings of 19th Coastal Engineering Conference,* Vol. II, American Society of Civil Engineers, 1715–1731.

IRIE, I.; KURIYAMA, Y., and ASAKURA, H., 1986. Study on scour in front of breakwaters by standing waves and protection methods. *Report, Port and Harbour Res. Inst., Japan,* 25(1), *4–86.*

JAFFE, B.E.; STERNBERG, R.W., and SALLENGER, A.H., 1984. The role of suspended sediment in shore normal beach profile changes. *Proceedings of Coastal Engineering '84,* 1983–1996.

KRAUS, N.C., 1988. The effects of seawalls on the beach: extended literature review. *Journal of Coastal Research,* Special Issue No. 4, 1–28.

KRAUS, N.C. and MCDOUGAL, W.G., 1996. The effects of seawalls on the beach: part 1, an updated literature review. *Journal of Coastal Research* 12(3), 691–701.

KRIEBEL, D.L., 1987. Beach recovery following Hurricane Elena. *Proceedings of Coastal Sediments '87,* American Society of Civil Engineers, 990–1005.

KRIEBEL, D.L.; DALLY, W.R., and DEAN, R.G., 1986. *Beach profile response following severe erosion events.* Coastal and Oceanographic Engineering Department, UF/COEL-86–016, University of Florida, Gainesville, FL.

LONGUET HIGGINS, M.S., 1953. Mass transport in water waves. *Phil. Trans. Royal Soc. London,* Series A, Vol 245, No. 903, 535–581.

MCDOUGAL, W.G.; KRAUS, N.C., and AJIWIBOWO, H., 1996. The effects of seawalls on the beach part II, numerical modelling of SUPERTANK seawall test. *Journal of Coastal Research* 12(3), 702–713.

MORTON, R.A., 1988. Interactions of storms, seawalls and beaches of the Texas coast. *Journal of Coastal Research,* Special Issue No. 4, 113–134.

MURRAY, P.B., 1992. *Sediment pick up in combined wave-current flow.* Unpublished Ph.D. Thesis, University of Wales, 189pp.

NAKASHIMA, L.D. and MOSSA, J., 1991. Responses of natural and seawall backed beaches to recent hurricanes on the Bayou Lafourche headland, Louisiana. *Z. Geomorph. N.F.* 35(2), 239–256.

NIELSEN, P., 1984. Field measurements of time averaged suspended sediment concentrations under waves. *Coastal Engineering* 8, 51–72.

PILKEY, O.H. and WRIGHT, H.L., 1988. Seawalls verses beaches. *Journal of Coastal Research,* Special Issue No. 4, 41–46.

RAKHA, K.A. and KAMPHIUS, J.W., 1995. A morphology model to predict erosion near a seawall. *Proceedings of Coastal Dynamics '95,* 879–890.

RUSSELL, P.E., 1993. Mechanisms for beach erosion during storms. *Continental Shelf Research,* 13(11), 1243–1265.

RUSSELL, P.; DAVIDSON, M.; HUNTLEY, D.; CRAMP, A.; HARDISTY, J., and LLOYD, G., 1991. The British Beach And Nearshore Dynamics (B-BAND) Programme. *Coastal Sediments '91,* 371–384.

SAWARAGI, T. and KAWASAKI, Y., 1960. Experimental study on behaviours of scouring at the toe of seadikes by waves. *Proceedings of 4th Japanese Coastal Engineering Conference,* Japan Society of Civil Engineers, 1–12 (in Japanese; figure and table captions in English).

SAYRE, W.O., 1987. Coastal erosion on the barrier islands of Pinellas County, West-Central Florida. *Proceedings of Coastal Sediments '87,* American Society of Civil Engineers, 1037–1050.

SEXTON, W.J. and MOSLOW, T.F., 1981. Effects of Hurricane David, 1979, on the beaches of Seabrook Island, South Carolina. *Northeastern Geology* 3(3/4), 297–305.

SILVESTER, R., 1977. The role of wave reflection in coastal processes. *Proceedings of Coastal Sediments '77,* American Society of Civil Engineers, 639–652.

SIMMONDS, D.; VOULGARIS, G., and HUNTLEY, D.A., 1995. Dynamic processes on a ridge and runnel beach. *Proceedings of Coastal Dynamics '95,* 868–878.

SOULSBY, R.L., 1990. Tidal-current boundary layers. *In:* LE-MEHAUTE, B. and HANES, D.M. (Editors), *The Sea,* (9B), Ocean Engineering Science. John Wiley & Sons, New York, 523–566.

SUMER, B.M. and FREDSOE, J., 2000. Experimental study of 2D scour and its protection at a rubble-mound breakwater. *Coastal Engineering,* 40(1), 59–87.

TATAVARTI, R.S.V.N., 1989. *The reflection of waves on natural beaches.* Unpublished Ph.D. Thesis. Dalhousie University, Halifax, Nova Scotia, Canada, 175pp.

TATAVARTI, R.V.S.N.; HUNTLEY, D.A., and BOWEN, A.J., 1988. Incoming and outgoing wave interactions on beaches. *Proceedings of 21st Conference on Coastal Engineering,* American Society Civil Engineers, 1104–1120.

TWU, S.W. and LIAO, W.M., 1999. Effects of seawall slopes on scour depth. *Journal of Coastal Research,* 15(4), 985–990.

XIE, S.L., 1981. *Scouring patterns in front of vertical breakwaters and their influence on the stability of the foundations of the breakwaters.* Department of Civil Engineering, Delft University of Technology, Delft, The Netherlands, 1–61.